

INTRODUCTION OF RARE EARTH ELEMENTS TO REPLACE SILICON IN THE USUAL COMPOSITION OF ULTRA-HIGH-TEMPERATURE CERAMICS

F. Rebillat^{1*}, A. S. Andreani¹, A. Poulon-Quintin²

¹University of Bordeaux, LCTS, 3 allée de la Boétie, Pessac, France

²ICMCB, CNRS, University of Bordeaux, 87 av. Dr. A. Schweitzer, Pessac, France

*rebillat@lcts.u-bordeaux1.fr

Keywords: solar furnace, dysprosium, oxidation mechanism.

Abstract

An original method for testing ultra-high-temperature ceramics (UHTC) at very high temperature (superior to 2200°C) in air with an exposure time of several minutes is used. The well known ZrB₂+SiC material shows a limited temperature of use in an oxidizing environment due to the too low stability above 2000°C of silica formed. A few new systems without silicon are proposed, starting from the Hf or Zr, C, B and rare earth elements. The choice of rare earths is motivated by the formation of oxides with melting points higher than 2000°C. The complex oxide scales formed during oxidation are accurately described, in term of presence of porosity and gradients of composition. Similarities with the mechanism of oxidation described for ZrB₂+SiC materials are shown. A significant higher thermal stability of rare earth oxide compared to silica is highlighted. As a consequence, the protection capacity of the oxide scale is improved.

1 Introduction

At very high temperature and in oxidizing atmosphere, zirconium and hafnium borides can be used as protective coatings of Carbon-Carbon composites [1-2]. ZrB₂ and HfB₂ compounds form, in oxidizing atmosphere at very high temperature (above 2000°C) porous solid oxides and a B₂O₃ liquid phase (melting point about 450°C). However, almost all B₂O₃ oxide evaporates at 1800°C [1]. In order to obtain a decrease of B₂O₃ liquid volatility, SiC is added to ZrB₂ or HfB₂. The aim is to form a borosilicate [2-3-4]. In literature, composition with 20vol% SiC has been identified in particular for its oxidation resistance [2-5]. However, the poor oxidation resistance of ZrB₂-SiC materials at very high temperature comes from the active oxidation of SiC. Further, the microstructure of ZrB₂-20vol% SiC (atomic Zr/Si ratio = 2.7) tested at T>2250°C, presents a low amount of protective silica associated to ZrO₂ and a SiC depletion zone in ZrB₂ close to the oxide/material interface, leading to a porous global structure and a brittleness of the material [6]. Often, only second phase silica and/or alumina formers are investigated [7-10], with a resulting oxidation resistance always limited by the poor thermal stability of silica at ultra high temperature.

This paper proposes a few new systems without silicon, starting from the Hf, C, B and Dysprosium systems. The choice of Dysprosium is motivated by the formation of oxides with melting points higher than 2000°C as well as their chemical affinity with B₂O₃ [11]. Thermal stability of this protective oxide scale formed by oxidation should be improved. The well

known self-healing process for the ZrB₂-SiC system is here expected to be maintained and to present higher chemical and thermal stabilities.

2 Experimental procedures

2.1 Elaboration

Samples are fabricated by Spark Plasma Sintering (SPS). The commercial powders used in this study are : HfB₂ (Neyco, particle diameter: 44 μm, purity: 99.5%), Hf (Alfa Aesar, particles diameter: 44 μm and purity: 99.6%), HfC (Alfa Aesar, particle diameter: 44 μm and purity: 99.5%) and DyB₄ (Cerac, particle diameter: 250 μm and purity: 99.6%). Sintering is done under high vacuum with heating conditions [7-8]: first a rise at temperatures 1300 or 1700°C with a ramp of 100°C.min⁻¹, then a dwell time for 5 min and lastly, a temperature decrease down to 600°C in 30 min. After elaboration, the samples dimensions are 5 mm height and 15 mm in diameter.

Different materials have been processed:

- with an initial atomic Hf/Dy ratio equal to 2.7 (in regard to Zr/Si in ZrB₂-20vol% SiC), fabricated from a mixture of Hf and DyB₄ powders, in order to observe the degradation evolution with the temperature increase,
- with a different initial atomic Hf/Dy ratio, fabricated from a mixture of Hf and DyB₄ powders, in order to observe the degradation evolution with the Hf/Dy ratio decrease (1.35) or increase (8.1 and 24.3),
- fabricated from a mixture of Hf carbide and DyB₄ powders, in order to observe the degradation evolution with the higher thermal stability of compounds initially used.

2.2 Oxidation test: solar furnace

For oxidation tests, sample surfaces are subjected to a constant solar flow of 15.5 MW.m⁻² for 3 min. A homogeneous Infra Red radiation is obtained on 1 cm². The temperature of surface material is measured by a monochromatic pyrometer calibrated for a surface emissivity of 1 (emissivity of HfC-SiC is between 0.85 and 0.95). Thus, the black body temperature ($T_{\text{black body}}$) given by the pyrometer is lower than the real sample temperature. When the solar flow is shuttered off, the cooling ramp is around 1000 °C.min⁻¹. The tests are realized in air with P_{H₂O} values (moisture content) ranging between 0.45 and 0.65 kPa.

2.3 Physical and chemical characterizations

The microstructures and the composition of samples are observed before and after oxidation tests (surfaces and cross-sections) and analyzed by Scanning Electron Microscopy (Quanta 400 FEG, FEI), by X ray Diffraction (PW 1820 Bragg Brentano geometry $\theta/2\theta$, Philips) and by Wavelength Dispersive X-ray Spectroscopy (WDS, Cameca SX 100).

3 Results

3.1 Density and initial microstructure

The sintering temperature is 1300°C and the final density is around 93% for all samples fabricated from Hf metallic powders. When Hf is introduced as carbide, the sintering temperature must be increased up to 1700°C. The final density is then around 85 %. The XRD analyses reveal the presence of various boride phases (DyB₄, HfB₂, DyB₂). A WDS quantitative analysis allows to verify the final atomic ratio obtained after SPS sintering. As expected, no volatilization of elements occurs during sintering. The size of grains remains similar to that of initial powders used.

3.2 Oxidation resistance of (Hf/Zr/Dy/B/C) materials at very high temperature

During oxidation of materials from the (Hf/Zr/Dy/B/C) system, the different phases expected to be formed are : a B₂O₃ liquid phase, a HfO₂ or ZrO₂ porous refractory oxide scale and Dy₂O₃, solid oxide at temperature up to 2000°C (T_{melting}=2340°C). Moreover, the solid compound, DyBO₃ formed, melts at 1585°C, and then the sealing liquid phase may be highly enriched in Dy₂O₃.


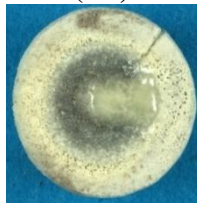


Material (Hf/Dy atomic ratio)	Hf+DyB ₄ (2.7)	Hf+DyB ₄ (2.7)	HfC+DyB ₄ (2.7)	HfC+DyB ₄ (1.35)
Optic observation of the top surface directly subjected to the solar flow				
T _{black body} (°C)	2250	2700	2200	2900
Mass variation, Δm	Δm>0	Δm>0	Δm>0	Δm=0
Consumed thickness (mm)	0.75±0.10	1.5±0.2	0.60±0.05	2.7±0.3
Thickness of the oxide scale (mm)	1.5±0.2	0.5±0.1	1.3±0.1	1.3±0.2

Table 1. Characterization of sample surfaces subjected to a constant solar flow of 15.5 MW.m⁻² for 3 min, in air, (a surface emissivity of 1 is fixed to give the black body temperature, T_{black body})

In the **Table 1**, only the test conditions realized on the Hf+DyB₄ (2.7) and HfC+DyB₄ (1.35 and 2.7) materials are presented, with a picture of sample surfaces after oxidation tests. For the others materials owning to Hf+DyB₄ system, we have observed:

- with the increase of the Hf/Dy atomic ratio (8.1 and 24.3), metallic hafnium becomes the main phase in the initial material, and his material has a poor refractory properties. Straight under the solar flow, the sample melts.
- with the decrease of the Hf/Dy atomic ratio (1.35), a catastrophic degradation of the sample due to the DyB₄ preferential oxidation is added to a relaxation of residual thermal stresses.

3.3 Oxidation test on Hf+DyB₄ (2.7) at T_{black body}=2250°C

The consumed thickness is 0.75±0.10 mm. The mass variation is positive. An observation of the cross section on the oxidized material is realized where the temperature was the highest. Many oxide layers are present. The WDS cartography realized on the cross section area where the temperature is the highest (**Figure 1 a** and **Figure 2**), highlights presence of different layers:

- The layer n°1 is 250±50 μm thick. Based on the XRD analysis realized on the top surface, DyBO₃ (JCPDS : 74-1933) is identified. WDS analyses on the cross section highlight an increase of the Dy content,
- The n°2 layer, porous (pores with a cylindrical shape and all oriented perpendicularly to the surface) and micro-cracked, is 1±0.1 mm thick. In this layer, the atomic ratio of oxygen is around 66% and 15±5% for boron. The distribution of Hf and Dy elements is inhomogeneous through this layer within the top part, with a Hf/Dy atomic ratio of 2±0.5 (the zone is Dy-enriched) and in the bottom part, a Hf/Dy atomic ratio equal to 2.7 (initial ratio),
- The n°3 layer is porous with small cylindrical pores compared to the n°2 layer and is 220±50 μm thick. The distribution of Hf, B and Dy elements is not anymore homogeneous.

The high Hf/Dy atomic ratio, 7 ± 1 , means that a departure of Dy occurs (as gaseous oxide species),

- The n°4 layer is $300 \pm 50 \mu\text{m}$ thick with a fine porosity. The distribution of Hf and Dy elements is homogeneous, in contrary to that of B and O elements. The Hf/Dy atomic ratio is unchanged (2.7 ± 0.5). Boron is mainly bonded to Hf, as HfB_2 phase. A preferential oxidation of dysprosium-containing compounds occurs.

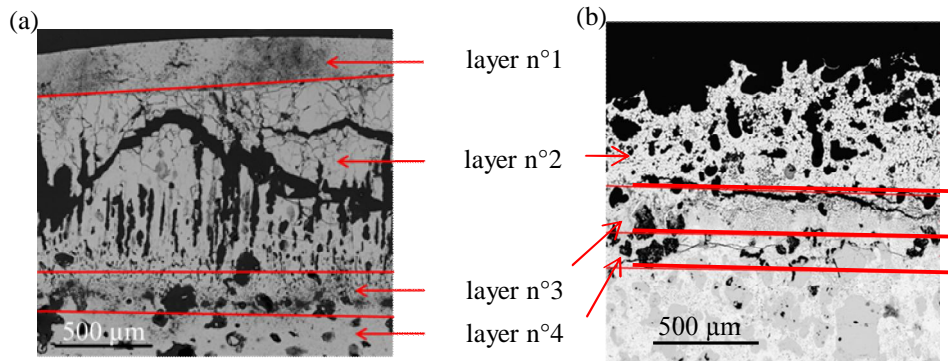


Figure 1. BSE -SEM image of samples cross sections after oxidation test in air, under a solar flow of $15.5 \text{ MW}\cdot\text{m}^{-2}$ (dwell time 3 min): (a) $\text{Hf}+\text{DyB}_4$ (2.7) ($T_{\text{black body}}=2250^\circ\text{C}$) and (b) $\text{HfC}+\text{DyB}_4$ (2.7) ($T_{\text{black body}}=2200^\circ\text{C}$)

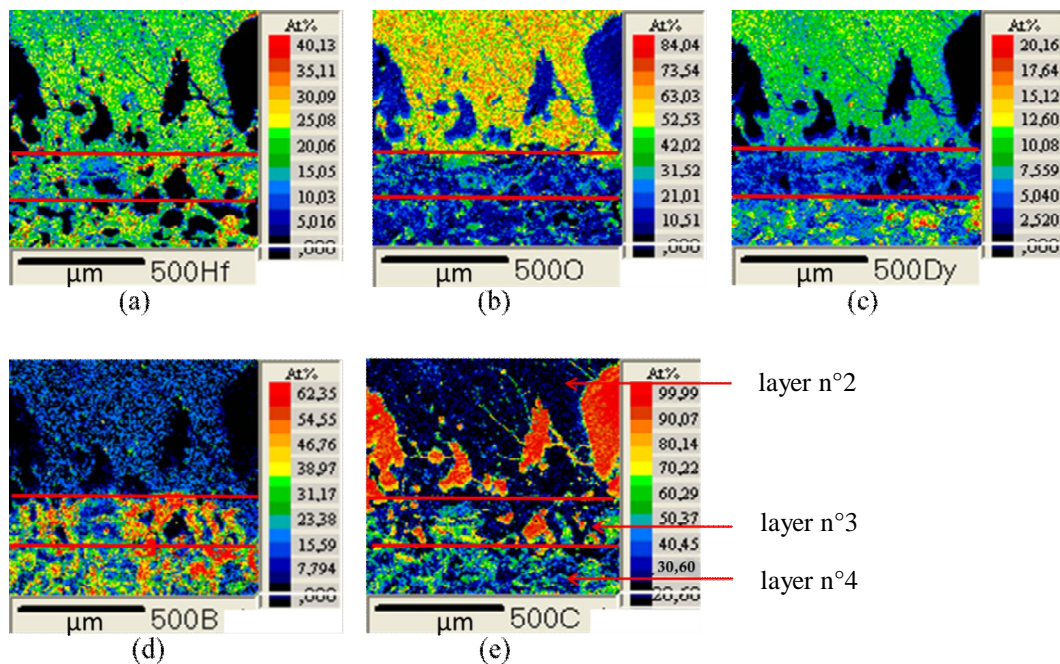
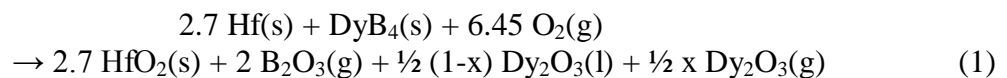


Figure 2. WDS mappings of: Hf, O, Dy, B and C elements after oxidation test of $\text{Hf}+\text{DyB}_4$ (2.7) ($T_{\text{black body}}=2250^\circ\text{C}$ in air, dwell time 3 min, under a solar flow of $15.5 \text{ MW}\cdot\text{m}^{-2}$)

B_2O_3 may be considered as fully volatilized. To get a positive mass variation, the quantity of Dy_2O_3 volatilized has to stay lower than 36 % (“x”: in reaction (1)) of the total Dy_2O_3 formed, according to the following global reaction (1).



The lower quantity of Dy at the oxide/material interface is due to its partial volatilization under a low oxygen partial pressure. Respectively, the enrichment in Dy_2O_3 is allowed into the top oxide layer, with a condensation of the gaseous species when the oxygen pressure

becomes higher. Moreover, with the formation of $\text{Hf}_2\text{Dy}_2\text{O}_7$, Dy_2O_3 should be stabilized at least until its melting point at 2700°C .

3.4 Oxidation test on $\text{HfC}+\text{DyB}_4$ (2.7) at $T_{\text{black body}}=2200^\circ\text{C}$

The consumed thickness is 0.60 ± 0.05 mm, value closed to that measured one for the $\text{HfC}+\text{DyB}_4$ (2.7) material (0.75 ± 0.1 mm). The propagation front of oxidation is parallel to the sample surface (**Figure 1 b**). A weight gain is measured.

On the cross section (**Figure 1 b** and **Figure 3**), only three layers are observed:

- The previous dense layer n°1 is not present,
- The layer n°2 is hugely porous. The average Hf/Dy atomic ratio is around 2.5 ± 0.5 . In contrary, close to the top surface, the quantity of dysprosium highly increases with a Hf/Dy atomic ratio reaching 1.2 ± 0.5 (Dy-enriched zone),
- The layer n°3, is as well porous. Dy is fully oxidized and mixed with HfC and HfB_2 . The Hf/Dy atomic ratio can locally reached a value as high as 3.5 ± 0.5 ,
- In the layer n°4, small pores are still present. The average Hf/Dy atomic ratio is unchanged (2.5). Dy is present in oxide as in boride phases.

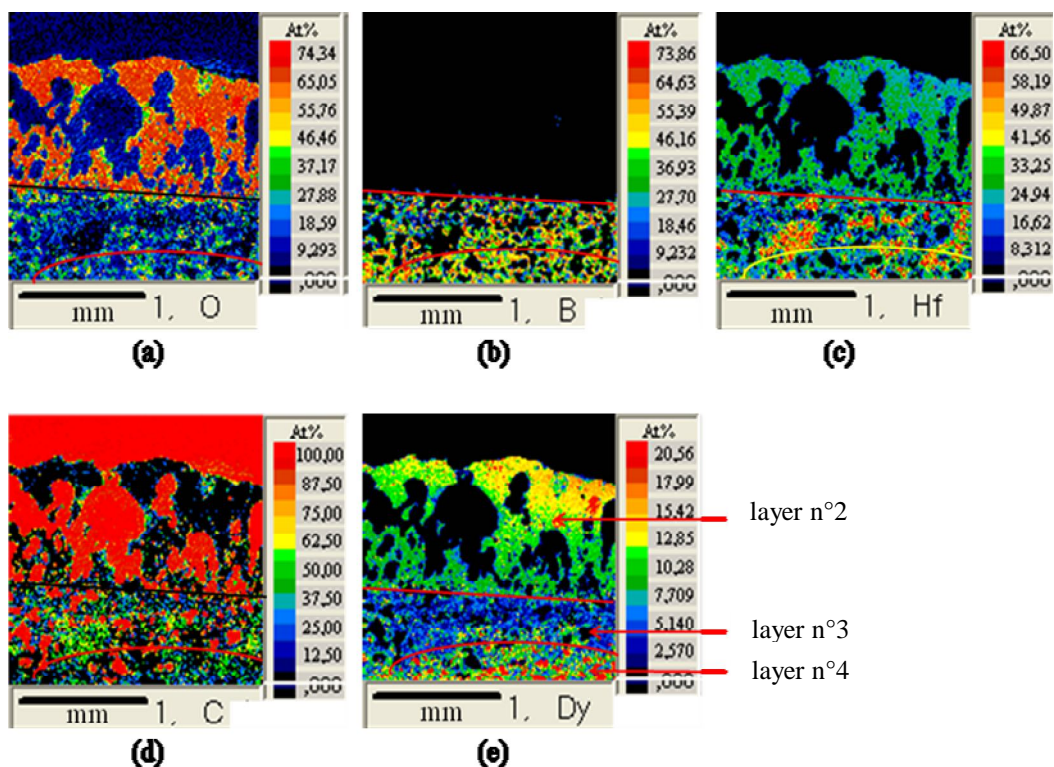


Figure 3. WDS mappings of: O, B, Hf, C and Dy elements after oxidation test of $\text{HfC}+\text{DyB}_4$ (2.7) ($T_{\text{black body}}=2200^\circ\text{C}$ in air, dwell time 3 min, under a solar flow of $15.5 \text{ MW}\cdot\text{m}^{-2}$)

3.5 Oxidation test on $\text{HfC}+\text{DyB}_4$ with different Hf/Dy ratio at ultra high temperature

The $\text{HfC}+\text{DyB}_4$ (1.35) material has been tested at ultra high temperature ($T_{\text{black body}}=2900^\circ\text{C}$). The consumed thickness is 2.7 ± 0.3 mm and the thickness of the formed oxide scale is 1.3 ± 0.2 mm (**Table 1**). The mass of the material is almost unchanged after the oxidation test. The observation of the cross section of the material shows the same succession of layers. However, the porosity is more important than in the $\text{HfC}+\text{DyB}_4$ (2.7) material.

According to the positive mass variation recorded after oxidation of $\text{HfC}+\text{DyB}_4$ (2.7), the residual present quantity of $\text{Dy}_2\text{O}_3(l)$ must be at least 82% of the $\text{Dy}_2\text{O}_3(l)$ formed oxide (similar estimation method to that previously used).

On the contrary, when the initial content of dysprosium boride is reduced, as in HfC+DyB₄ (8.1), the samples exploded under the solar thermal flow, with a radial cracking process. This failure is related to a problem of too intense thermal residual stress coming from the SPS sintering, generally observed for sample with a high quantity of carbides.

4 Discussion

Figure 4 summarized the three mechanisms of oxidation for the ZrB₂ + SiC (2.7), Hf+DyB₄ (2.7) and HfC+DyB₄ (2.7) considered systems.

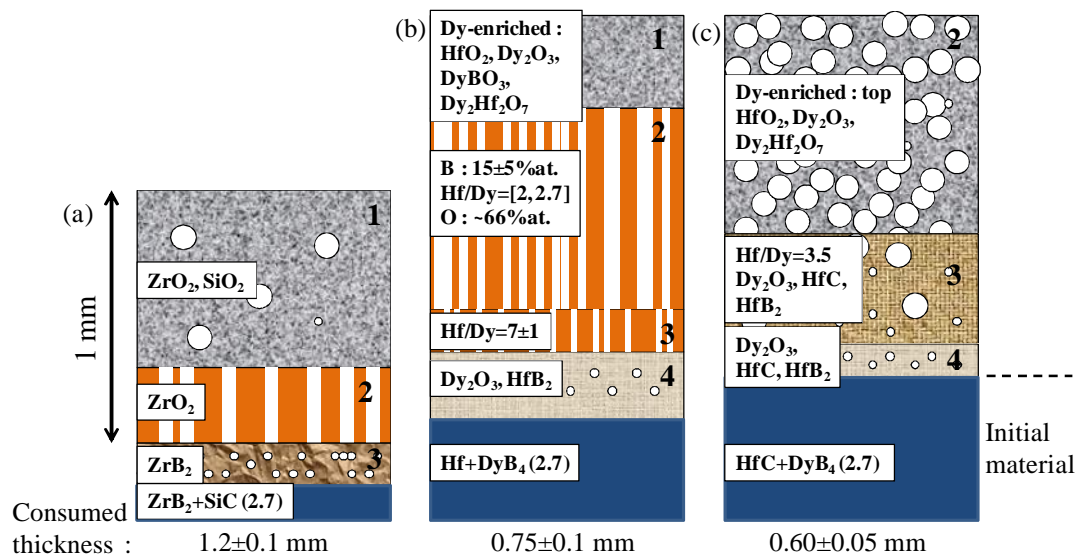


Figure 4. Schematic representation of oxidation mechanism for $T_{\text{black body}} \approx 2200^{\circ}\text{C}$ in air and for 3 min: (a) ZrB₂+SiC (2.7) , (b) Hf+DyB₄ (2.7) and (c)HfC+DyB₄ (2.7)

With the introduction of metallic Hf in the (Hf/B/Dy) system, the SPS sintering is easier, leading to a more compact material. But the refractoriness of these materials is not sufficient as soon as the Hf/DyB₄ molecular ratio is higher than around 8.

With the use of metallic Hf, the growth of HfO₂ is columnar.

The formation of Hf₂Dy₂O₁₇ may allow thermally and chemically partially stabilizing Dy₂O₃. However, Dy₂O₃ possesses a lack of thermo-chemical stability under low oxygen partial pressure at high temperature. Its volatilization should occur at the oxide/material interface. But, its condensation close to the top surface of the oxide layer is due to the higher oxygen partial pressure. The departures of gaseous boron and dysprosium containing species may initiate the formation of porosities at the oxide/material interface and in the oxide layer.

For temperatures close to 2200°C in air, the higher is the refractoriness of the material; the lower is the consumed thickness by oxidation (**Figure 4** b and c). The introduction of carbide (HfC+DyB₄ (2.7) material) allows to enhance the refractoriness of the system and to increase the allowed temperature of use. Indeed, dysprosium and hafnium are both fully stabilized as refractory carbide and/or boride. The previous mentioned columnar structure of HfO₂ is completely destroyed when HfC is used, certainly in relation with the higher quantity of formed gaseous species (CO, CO₂) added to B₂O_{3(g)}. The important departure of formed gases should impose a limited time of exposure to very high temperatures (**Figure 4** c).

Anyway, the formation of Dy₂O₃, instead of SiO₂, brings a significant improvement of the thermal stability of the protective oxide scale formed during oxidizing aging. At the end of all the tests, the residual quantity of Dy₂O₃ remains at least around 80 % of the whole amount of formed Dy₂O₃.

Although, chemical interactions may be act between Dy_2O_3 and B_2O_3 since solid compounds are formed at lower temperatures, B_2O_3 is not significantly thermally stabilized.

For comparison, in similar conditions, for $ZrB_2 + SiC$ system (with a 20 % volume ratio of SiC or a Zr/Si ratio equal to 2.7), for the extreme top surface, where the oxygen pressure is higher, a liquid silica formation occurs. The evaporation of boron oxide is total. Close to the non oxidized material, a porous layer mainly constituted of ZrB_2 is present due to the whole active oxidation of SiC (**Figure 4.a**).

At very high temperature ($T > 2400^\circ C$), the introduction of dysprosium as a refractory boride in the ($Hf + DyB_4$) and ($HfC + DyB_4$) systems allows to bring a liquid phase during oxidation. This liquid phase can fill the porosities at the top surface of the HfO_2 refractory porous skeleton, like SiO_2 for the $ZrB_2 + SiC$ system. Then, the oxygen diffusion is limited. Due to the higher temperature, the consumed thickness is around twice those previously measured. The layering of the oxide scale under the solidified liquid phase over the top surface remains very similar. The whole oxide thickness is respectively thinner. At the end of the test, the measured weight gain again proves the higher thermal stability of Dy_2O_3 compared to that of SiO_2 .

For comparison, in similar conditions, for $ZrB_2 + SiC$ system (with a 20 % volume ratio of SiC or a Zr/Si ratio equal to 2.7), the consumed thickness of material reaches 3 mm. For temperature higher than $2400^\circ C$, silica is catastrophically thermo chemically instable. The active oxidation of SiC is accelerated and the large SiC depletion zone formed (2 mm thick) in ZrB_2 is extremely brittle and porous due to SiO, CO/CO₂ gas evacuation.

5 Conclusion

For materials owing to the (Hf, Dy, B, C) system, the complex oxide scales formed during oxidation, at temperature above $2200^\circ C$, are accurately described, mainly in term of presence of porosity and gradients of composition. Respectively, the thicknesses of consumed material increases with the temperature of test, as the thicknesses of formed oxide decreases, due to more important volatilization phenomenon. The higher is the refractory properties of the material and the thinner is its consumed thickness. The oxidation mechanism (above $2200^\circ C$) shows similarities with those widely described for $ZrB_2 + SiC$ materials, at temperature below $2000^\circ C$. Respectively, the studied materials show a mass gain during oxidation, instead of a weight lost generally registered for the $ZrB_2 + SiC$ system (Zr/Si ratio = 2.7), due to the active oxidation of SiC. Thus, a significant higher thermal stability of Dy_2O_3 compared to SiO_2 is proved and the protection capacity of the oxide scale is significantly enhanced at very high temperatures. Further works should be done on thermodynamic calculations to estimate equilibrium partial pressures of gases over these kinds of materials.

Acknowledgments

This work has been supported by the Aquitaine country (Région Aquitaine) and Snecma Propulsion Solide (SPS) through a grant given to A.S. Andréani. The authors are grateful to E. Guillot (Research engineer, Solar furnace installation, CNRS, PROMES UPR 8521, Font Romeu, France) for the tests in the solar furnace of Font Romeu, Dr. C. Estournès (CNRS, Plate-forme Nationale de Frittage Flash, PNF2-CNRS, Module de Haute Technologie, University Paul Sabatier, Toulouse, France) for the processing of samples by Spark plasma sintering, M. Lahaye for assistance with EPMA analyses and the resources center XRD, CNRS, ICMCB, University of Bordeaux, France.

References

- [1] Parthasarathy T.A., Rapp R.A., Opeka M., Kerans R.J. A model for the oxidation of ZrB₂, HfB₂ and TiB₂. *Acta Materialia*, **55**, pp. 5999-6010 (2007).
- [2] Opeka M.M., Talmy I.G., Zaykoski J.A. Oxidation-based materials selection for 2000°C+hypersonic aerosurfaces : Theoretical considerations and historical experience. *Journal of materials sciences*, **39**, pp. 5887-5904 (2004).
- [3] Han J., Hu P., Zhang X. oxidation-resistant ZrB₂-SiC composites at 2200°C, Composites Science and technology. *Composites Science and technology*, **68**,799-806 (2008).
- [4] Levine S.R., Opila E.J., Halbig M.C., Kiser J.D., Singh M., Salem J.A. Evolution of ultra-high temperature ceramics for aeropulsion use. *Journal of the European Ceramic Society*, **22**, pp. 2757-2767 (2002).
- [5] Johnson S. Processing, properties and arc jet oxidation of hafnium diboride/silicon carbide ultra high temperature ceramics. *Journal of materials science*, **39**, pp. 5925-5937 (2004).
- [6] Andreani A-S., Rebillat F., Poulon-Quintin A. Oxidation mechanism of ZrB₂-SiC tested in a solar furnace above 2200°C. *High Temperature Ceramic materials and Ceramics*, edited by W. Krenkel and J. Lamon, ISBN 978-3-00-032049-1, pp. 840-845 (2010).
- [7] Sciti D., Balbo A., Bellosi A., *Journal of the European Ceramic Society*, **29**, 1809 (2009)
- [8] Li G., Han W., Zhang X., Han J., Meng S. Ablation resistance of ZrB₂-SiC-AlN ceramic composites. *Journal of Alloys and Compounds*, **479**, pp. 299-302 (2009).
- [9] Chen G., Zhang R., Hu P., Han W. Oxidation resistance of Zr₂(Al(Si))₄C₅-based composites at ultra-high temperature. *Scripta Materialia*, **61**, pp. 697-700 (2009).
- [10] Sciti D., Silvestroni L., Celotti G., Melandri C., Guicciardi S. Sintering and mechanical properties of ZrB₂-TaSi₂ and HfB₂-TaSi₂ ceramic composites. *Journal of the American Ceramic Society*, **91** (10), pp. 3285-3291 (2008).
- [11] Phase Diagram for Ceramics. compiled at the *National Institute of Standards and Technology*, edited and published by the *American Ceramic Society*.